# Renewable OME from biomass and electricity—Evaluating carbon footprint and energy performance

N.B. When citing this work, cite the original published paper.

(article starts on next page)
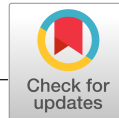
**RESEARCH ARTICLE**

# Renewable OME from biomass and electricity—Evaluating carbon footprint and energy performance

Pontus Bokinge[1] [iD] | Stefan Heyne[1] | Simon Harvey[2]

[1]CIT Industriell Energi AB, Göteborg, Sweden

[2]Energy Technology, Department of Space, Earth and Environment, Chalmers University of Technology, Göteborg, Sweden

**Correspondence**
Pontus Bokinge, Sven Hultins Plats 1-2, SE-412 88 Göteborg, Sweden.
Email: pontus.bokinge@chalmersindustriteknik.se

## Abstract

Renewable drop-in fuels provide a short- to medium-term solution to decreasing carbon dioxide emissions from the transport sector. Polyoxymethylene ethers (OME) are among interesting candidates with production pathways both from biomass (bio-OME) as well as electricity and $CO_2$ (e-OME) proposed. In the present study, both bio- and e-OME production via methanol are assessed for energy performance and carbon footprint. Process integration methods are applied to evaluate synergies from colocating methanol production with further conversion to OME. Even a hybrid process, combing bio- and e-OME production is evaluated. The energy efficiency of bio-OME is considerably higher than for the e-OME pathway, and colocation synergies are more evident for bio-OME. Carbon footprint is evaluated according to EUs recast Renewable Energy Directive (RED II). If renewable electricity and natural gas are used for power and heat supply, respectively, results indicate that all pathways may be counted toward the renewable fuel targets under RED II. The largest emissions reduction is 92.8% for colocated hybrid-OME production. Carbon footprints of e- and hybrid-OME are highly sensitive to the carbon intensity of electricity, and the carbon intensity of the heat supply has a major impact on results for all pathways except colocated bio- and hybrid-OME.

**KEYWORDS**
biofuels, e-fuels, GHG emissions, polyoxymethylene ethers, process integration, renewable transportation fuels

## 1 | INTRODUCTION

The European Union (EU) is—in line with the Paris Agreement—striving for drastic reductions of greenhouse gas (GHG) emissions within all sectors. For the transport sector, a goal of 20% reduction in GHG emissions in relation to 2008 level, and 60% reduction by 2050 with respect to 1990 is aimed at.[1] On a shorter timeframe, the recently revised Renewable Energy Directive (RED II) states that at least 14% of fuel in transportation must be from renewable sources by 2030. To be counted toward the RED II target, biofuels and nonbiofuels must achieve emission reductions of 65% and 70%, respectively, compared to fossil fuels. A major track for GHG reduction is electrification of the light duty vehicle fleet, but renewable fuels from biomass and/or renewable electricity are also acknowledged to play an important role in the transition to a sustainable transport sector (eg,[2,3]). Renewable fuels that can be used as drop-in fuels in

the current vehicle fleet play an important role in reducing greenhouse gas emissions from the transportation sector in a short to medium term. Both fuels based on biomass and renewable electricity can contribute to the reduction. There are a number of research initiatives looking at advanced renewable fuel alternatives that combine sustainable production pathways with excellent combustion properties, resulting in low combustion emissions and good well-to-wheel environmental performance. Examples for such initiatives are Co-Optima in the United States,[4] the Fuel Science Centre in Aachen/Germany[5] or the Future Fuel project in Sweden[6] that the present work is part of. König et al[7] published an extensive screening of different renewable fuel alternatives, considering biomass or renewable electricity as main process input, as well as hybrid process concepts. They conclude that biomass-based fuels are a cost-efficient way of producing renewable fuels but have a low carbon efficiency. Electro-based fuels on the other hand are stated to come at a high production cost but allow for almost complete conversion of the feedstock carbon to fuel product. They also conclude at the example of ethanol production, that—in order to cover a given fuel demand—a fleet of hybrid electro-bio-plants is a preferable option to a combination of biomass-only and electrofuel plants with respect to the pareto-optimality between cost efficiency and carbon loss.[7] Poulikidou et al[8] investigated the lifecycle energy balance and GHG emissions for three different production pathways for 2-ethylhexanol, an advanced bio-based drop-in diesel fuel. They combined information from production energy and GHG performance with engine experimental tests to come up with lifecycle energy and greenhouse gas performance. 2-Ethylhexanol is stated to provide a competitive alternative to fossil transport fuels, with in particular the pathway from biomass gasification via syngas performing well from both an energy and GHG emission perspective.

A renewable drop-in fuel for diesel engines receiving considerable attention recently is polyoxymethylene ether (OME).[9-19] Other abbreviations that are used for polyoxymethylene ethers in literature include POMDME, PolyDME, $OMDME_n$, $DMM_n$, or $PODE_n$. It can either be a pure fuel consisting of, for example, dimethoxymethane (DMM), also called methylal—$OME_1$—or a mixture of ethers with varying chain length, the most common mixture investigated as renewable fuel replacing fossil diesel being $OME_{3-5}$. This mixture is the focus of the present work and is preferred because diesel-$OME_{3-5}$ blends are expected to comply with European fuel standards (EN 590) and require only minor modifications to fuel and engine infrastructure.[20,21] For shorter chain lengths (n < 3), flash points are too low, while longer chain lengths (n > 5) have negative impact on cold flow properties.[22,23] Longer chain lengths (up to n = 8) may however be acceptable to some extent in higher temperature grade diesels.[22] The mixture of $OME_n$ with n = 3-5 is miscible with

diesel to a large fraction, and even possible to use as pure fuel.[12,24-26] A major benefit identified for OME in comparison with fossil diesel as a fuel is the possibility of achieving simultaneous reduction in soot and $NO_x$ emissions that is difficult to obtain with fossil diesel.[12] The reduction is considered to be primarily related to the oxygen content of the fuel (in the range of 48 wt-% for $OME_{3-5}$ blends). This higher oxygen content however also implies a reduced energy content (lower heating value (LHV) of about 19 MJ/kg for $OME_{3-5}$ vs ca. 43 MJ/kg for fossil diesel) and associated drawbacks in energy density, respectively, driving range when considering the use in vehicles. Nevertheless, given the considerable reduction of particulate matter and $NO_x$ emissions in combination with production processes from renewable energy, $OME_{3-5}$ is considered a promising option for contributing to reduced GHG emissions from the transportation sector.

The production of $OME_n$ from methanol has been studied in detail by, for example,[17-18,27-32] focusing on the entire process or individual process steps, and with most studies targeting $OME_{3-5}$. Production commonly proceeds via formaldehyde, using either a direct (eg,[18]) or an indirect route (eg,[17,27,31,32]). For the direct route, formaldehyde and methanol are directly converted to $OME_n$ while for the indirect route, the conversion of formaldehyde and methanol proceeds via intermediates trioxane and methylal. Alternatively, some researchers suggest production via para-formaldehyde as an intermediate instead of trioxane (eg,[21,33,34]), thus avoiding costly and energy-intensive trioxane production.[34] In most process concepts, off-spec OMEs and unreacted educts are recycled and the process has no value-added by-products. If recycling is used, product yields are very similar between processing routes, but the energy demand differs to some extent and the number of processing units for the direct conversion route is considerably smaller, presumably leading to decreased investment cost. The differences between the different routes are discussed in more detail in References 17,21,35.

Recently, Held et al[35] published mass and energy balances, as well as stream data, for the entire production process chain from methanol to $OME_{3-5}$, following the direct route and the indirect route (via trioxane) described above. Held et al[35] also evaluate the energetic efficiency of an electrofuel production concept in which the methanol required for $OME_{3-5}$ production is synthesized from electrolysis-based hydrogen and $CO_2$ provided via carbon capture. In their analyses, heat recovery is optimized using pinch analysis and several levels of process integration are considered. Their results show that, if the required $CO_2$ is captured from flue gases, the production of 1 MJ $OME_{3-5}$ (LHV 19.2 MJ/kg) requires about 2.7 MJ of electric power and 0.2-0.4 MJ of heat, depending on the level of heat integration and on the process route employed for conversion of methanol to $OME_{3-5}$. This corresponds to an energetic efficiency of roughly 32%-34%, the most

significant energy loss being associated with the electrolysis unit. Considering the high electricity demand, which is almost entirely due to hydrogen production, a potential process improvement is to produce formaldehyde by direct hydrogenation of methanol—generating hydrogen as a by-product—rather than by the commonly used oxidative processes.[36] According to estimates in,[35] this can reduce power demand by up to 0.5 MJ/MJ $OME_{3-5}$ at the expense of increased heat demand. Due to a lack of detailed process data, this alternative was however not investigated further by.[35]

An almost identical electrofuel production concept—using carbon capture from flue gases and $OME_{3-5}$ production by the indirect formaldehyde route—was recently evaluated by[33] who determined the exergetic efficiency to 38%, corresponding to an energetic efficiency (using the same metric as was used by[35]) of 30%. The lower energetic efficiency—compared to[35]—is mainly due to a higher heat demand. However, thermal stream data and details on the parameters used in pinch analysis (in particular, the value of the minimum temperature difference) were not published by,[33] making an in-depth comparison difficult.

Studies on OME production from biomass are scarce, but one process configuration based on biomass gasification followed by syngas upgrading and methanol synthesis was developed by A. Kumar et al.[13,19,37] The product of the proposed process is $OME_{1-8}$ meaning it contains both longer and shorter OME chains and, moreover, the yield of the process employed for conversion of methanol to OME is low compared to other literature. Mass yield is about 38% for $OME_{1-8}$ and 11% for $OME_{3-5}$, based on feed methanol. This can be compared to the process developed by Burger et al[27]—and used in the electrofuel production concept described above—achieving almost 80% $OME_{3-5}$ mass yield. The difference in yield is likely explained by the fact that Kumar et al consider a single pass process, while reactors in the process developed by Burger operate with recycle of unconverted educts and side-products. Because of the low yield, the process by Kumar et al is assumed to underestimate the attainable yield in OME production from biomass. However, several studies investigate methanol production from biomass (see for example[38-43]) and can be combined with the methanol to $OME_{3-5}$ process described in (eg,[27-28,35]) to arrive at a complete biomass to $OME_{3-5}$ process.

The aims of the present work were to analyze and compare $OME_{3-5}$ production based on biomass, electricity, and $CO_2$, as well as based on a hybrid concept. The mass and energy balances for methanol synthesis and the further conversion to $OME_{3-5}$ are established based on existing literature data. Process integration tools are used to assess synergies from colocating methanol and $OME_{3-5}$ production, as well as cogeneration of electricity from available excess heat from the processes. The energy efficiency as well as the greenhouse gas reduction potential in relation to fossil diesel is assessed.

## 2 | METHODOLOGY

The present work analyses energy and GHG emissions performance of six different process pathways for $OME_{3-5}$ production. All pathways proceed via the platform chemical methanol, and three options for methanol synthesis and two options for the synthesis of methanol to $OME_{3-5}$ are considered. Methanol is produced either from biomass (bio-methanol), from $CO_2$ and electricity (e-methanol), or using a hybrid concept (hybrid-methanol). In the hybrid concept, a separated $CO_2$ stream which is intrinsic to the bio-methanol process is fed to the e-methanol process. Methanol is subsequently converted into $OME_{3-5}$ using either a direct route or an indirect route via trioxane as described above. Due to a lack of process data—especially detailed thermal stream data—the abovementioned route via para-formaldehyde is not considered in the present work. Off-spec OMEs and unreacted educts in the OME reactor effluent are recycled to the reactor inlet, and the process has no value-added chemical by-products. Below, the different process concepts are referred to as bio-$OME_{3-5}$, e-$OME_{3-5}$, or hybrid-$OME_{3-5}$, depending on the pathway used for methanol production.

For bio-based $OME_{3-5}$ (bio-$OME_{3-5}$) production, methanol is assumed to be produced from biomass via the process described in,[42,43] involving oxygen-blown biomass gasification followed by water-gas shift, $CO_2$ removal and methanol synthesis. For $OME_{3-5}$ production from electricity and $CO_2$ (e-$OME_{3-5}$), it is assumed that methanol is synthesized using $CO_2$ captured from flue gases and $H_2$ produced by water electrolysis, as described in Held et al.[35] In the hybrid concept (hybrid-$OME_{3-5}$), the $CO_2$ separated from bio-methanol is used to produce e-methanol. It is assumed that the hybrid process will make use of the entire $CO_2$ stream from the bio-based process and that no additional $CO_2$ will be supplied, meaning that the carbon capture unit used in the e-$OME_{3-5}$ process is not used in the hybrid process. Additionally, oxygen for the biomass gasification plant is supplied from the electrolysis plant, eliminating the need for the on-site air separation unit (ASU) and reducing the process electricity demand.

The process steps used for conversion of methanol to $OME_{3-5}$ are the same for all process concepts (bio-, e-, or hybrid-$OME_{3-5}$). As discussed above, both a direct and an indirect route have been proposed for methanol to $OME_{3-5}$ conversion. Below, the performance of each process concept (bio-, e-, and hybrid-$OME_{3-5}$) is assessed considering both the direct and the indirect route (referred to as route A and B, respectively). The different process configurations are illustrated in Figure 1.
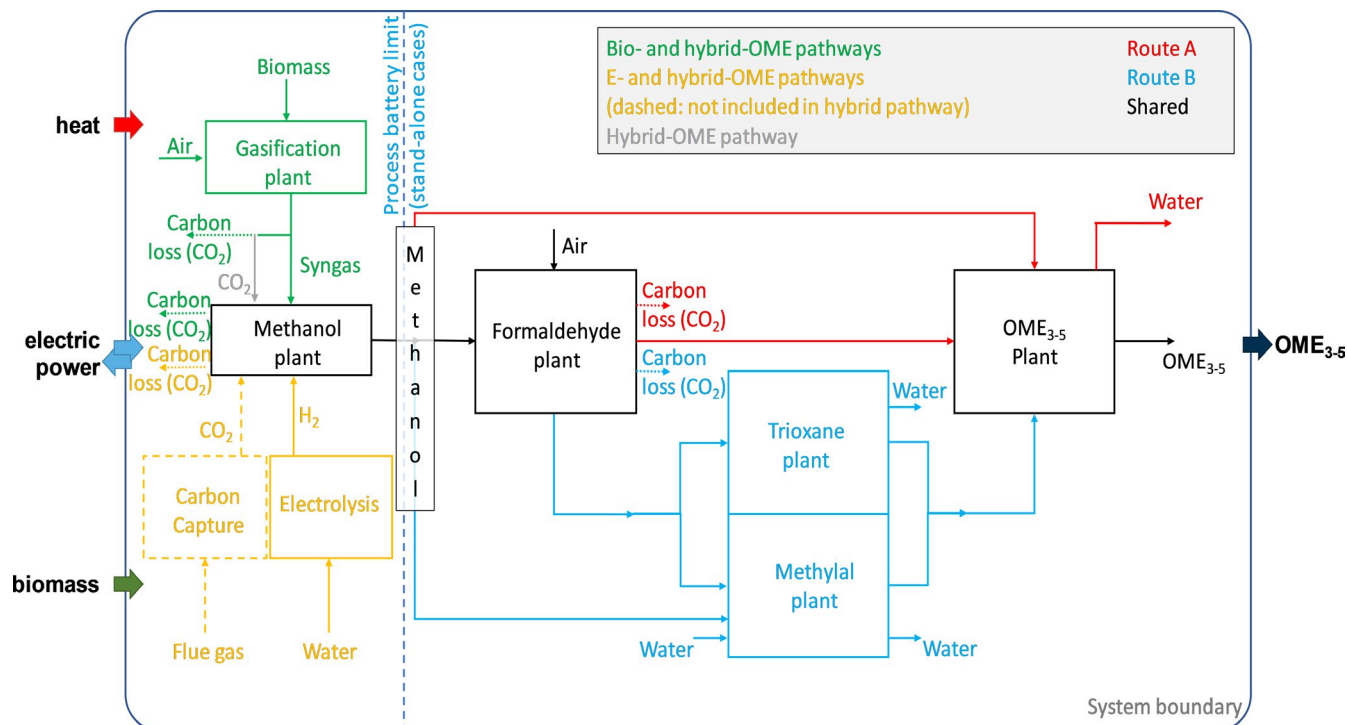
**FIGURE 1** Considered OME$_{3-5}$ process configurations and system boundary for energy efficiency and GHG emission assessment. The hybrid-OME$_{3-5}$ pathway combines processes and streams from the bio-OME$_{3-5}$ (green) and e-OME$_{3-5}$ (yellow) pathways. Dashed lines represent streams or process steps which are not present in the hybrid process. Dotted lines represent carbon loss from processing steps (basically CO$_2$). In the hybrid process, an almost pure CO$_2$ stream (dotted green line) separated from the biomass-based syngas stream is used for methanol production (solid gray line) instead of CO$_2$ from carbon capture (dashed yellow line)

**TABLE 1** Feedstock, methanol to OME$_{3-5}$ conversion route, and level of heat integration for the different OME$_{3-5}$ production pathways investigated

| Case | Feedstock | MeOH to OME$_{3-5}$ conversion | Level of heat integration |
|---|---|---|---|
| Bio-OME-A-SA | Biomass | Route A | Stand-alone |
| Bio-OME-A-Int | | Route A | Integrated |
| Bio-OME-B-SA | | Route B | Stand-alone |
| Bio-OME-B-Int | | Route B | Integrated |
| e-OME-A-SA | CO$_2$ and water (hydrogen) | Route A | Stand-alone |
| e-OME-A-Int | | Route A | Integrated |
| e-OME-B-SA | | Route B | Stand-alone |
| e-OME-B-Int | | Route B | Integrated |
| Hybrid-OME-A-SA | Biomass and water (hydrogen) | Route A | Stand-alone |
| Hybrid-OME-A-Int | | Route A | Integrated |
| Hybrid-OME-B-SA | | Route B | Stand-alone |
| Hybrid-OME-B-Int | | Route B | Integrated |

For each process configuration, the net energy input of biomass, heat, and power required to produce one MJ of OME$_{3-5}$ is evaluated. Process yields, power demand, and thermal stream data are gathered from the underlying publications for each process concept (see below). Pinch analysis—a widely used method to determine the minimum heating and cooling demand of various industrial processes and to identify potential process energy efficiency

improvements[44,45]—is used to establish the minimum heating demand, and two cases are considered for heat integration. Case "Integrated" represents a fully integrated process chain, where the entire production from feedstock to OME$_{3-5}$ is located at the same site and heat exchange between all process streams is allowed. Case "Stand-alone" represents a separated process chain, where the feedstock to methanol process is physically separate from the methanol to OME$_{3-5}$

process, meaning no heat integration between the two parts of the process is possible (dashed blue line in Figure 1). Combined with the six different process configurations, two levels of heat integration result in twelve cases for energy analysis. These are summarized in Table 1 below. For process concepts involving biomass gasification (bio- and hybrid-$OME_{3-5}$), high temperature excess heat is available and utilization of this heat to raise steam for cogeneration of heat and power has been considered. In these cases, the power generation target has been established using pinch analysis. The power generation is balancing the power demand of the different pathways, resulting in a net power demand/generation for each case.

Process yields, power demand, and thermal stream data for methanol production based on oxygen-blown biomass gasification is based on.[42,43] For the subsequent conversion of methanol to $OME_{3-5}$, the data published by Held et al[35] for e-$OME_{3-5}$ has been used. This means that the methanol to $OME_{3-5}$ conversion is the same for bio-, e-, and hybrid-$OME_{3-5}$. Data have been gathered from the underlying publications and used without modifications other than scaling to 1 MW of $OME_{3-5}$ output (based on LHV: 19.2 MJ/kg[a]).

Energy demand data for e-$OME_{3-5}$ production are taken directly from Held.[35] Note that the minimum heating demand is already evaluated by Held et al[35] using pinch analysis. The same levels of integration (ie, methanol production separated from or colocated with $OME_{3-5}$ production) and the same production routes (direct and indirect) are analyzed, allowing for a direct use of the results in the present work. Held et al[35] consider different options for $CO_2$ supply, and the numbers used in the present work refer to $CO_2$ captured from flue gases.

The assessment of the hybrid-$OME_{3-5}$ process combines data for the bio- and e-$OME_{3-5}$ processes. As mentioned above, it is assumed that the entire $CO_2$ stream from the bio-$OME_{3-5}$ process is fed to the e-$OME_{3-5}$ process and that no additional $CO_2$ is supplied. In the hybrid concept, oxygen from the electrolysis plant satisfies the oxygen demand of biomass gasification plant and, consequently, the power demand of the ASU used to supply oxygen in the bio-$OME_{3-5}$ process is eliminated.

In order to evaluate the process concepts from an energy efficiency perspective based on the system boundaries indicated in Figure 1, the following definition is used.

$$\eta = \frac{\sum_o \dot{m}_o \cdot LHV_o + \dot{Q}^- + \dot{W}_{el}^-}{\sum_i \dot{m}_i \cdot LHV_i + \dot{Q}^+ + \dot{W}_{el}^+} \quad (1)$$

with $\dot{m}$ being the mass flow, $LHV$ the lower heating value, $\dot{Q}$ heat flow, and $\dot{W}_{el}$ electricity for the respective streams. The subscripts and superscripts denote outputs ("$-$") and inputs ("$+$"), respectively. Only net flows are considered

when evaluating the energy efficiency definition, implying that terms for heat and electricity only contribute to either the nominator or denominator of the right-hand side of Equation (1). In contrast to the GHG emission evaluation, no transport operations are accounted for in the definition of the energy efficiency $\eta$.

The GHG emission evaluation is done on a well-to-tank perspective according to Annex V of the recently updated Renewable Energy Directive (RED II) of the European Commission.[46] Default values for more established biofuel production pathways are included in Annex V and Annex VI of RED II and have been calculated using input data defined in a 2019 report by the European Commission's Joint Research Centre (JRC).[47] To allow for comparison with default values given in RED II, for example, FT-diesel, the same input data have been used in the present work. Energy allocation is used in accordance with RED II guidelines to account for cogeneration of electricity. RED II dictates that the carbon intensity of electricity imported from the grid is taken as the regional grid average but allows for using the carbon intensity of an individual plant in case of a direct connection to the production process. In the base case of the present work, electricity is assumed to be supplied by a wind farm (0 g $CO_{2eq}$/MJ power). Heat demand is assumed to be covered by firing of natural gas in a utility boiler at 90% thermal efficiency (related to fuel LHV). With a carbon intensity of 65.9 g $CO_{2eq}$/MJ for natural gas (including provision and combustion),[47] the resulting carbon intensity of heat supply is 73.2 g $CO_{2eq}$/MJ. Other options for heat and power supply are considered in sensitivity analyses.

Emissions associated with transportation of feedstock, intermediates, and final products are estimated according to the guidelines given in Section 5 in the JRC report underlying the RED II default emission values.[47] Biomass feedstock is assumed to be transported 300 km by road, and for stand-alone process configurations, the methanol intermediary is assumed to be transported 150 km by road. 40 ton diesel trucks with a 27 ton payload are assumed to be used for all road transports. For the biofuel pathways included in Annex V of RED II, the transport mix given in Table 2 below is assumed for final distribution. The same transport mix is used for GHG emission calculations in the present work.

Input biomass is assumed to be wood chips from forest residues and $CO_2$ emissions associated with cultivation and processing are taken from Annex V of the RED II.

The final use of $OME_{3-5}$ is assumed to be carbon neutral for all cases and the GHG emission reduction is calculated with reference to fossil diesel use, having a baseline value of 94 g $CO_{2eq}$/MJ.[46]

Detailed GHG emission calculations are available in the Appendix S1.

| | Transport | Share | Distance (km one way) |
|---|---|---|---|
| To blending depot | Truck (payload 27 t) | 13.2% | 305 |
| | Product tanker (payload 15 000 t) | 31.6% | 1118 |
| | Inland ship (payload 1200 t) | 50.8% | 153 |
| | Train | 4.4% | 381 |
| From blending depot to filling station | Truck (payload 27 t) | 100% | 150 |

**TABLE 2** The transport mix assumed for final distribution of $OME_{3-5}$

**TABLE 3** Carbon yield and mass flow rates of important streams for the six production pathways

| | Bio-OME | | e-OME | | Hybrid-OME | |
|---|---|---|---|---|---|---|
| | Route A | Route B | Route A | Route B | Route A | Route B |
| Carbon yield [%] | 38.0 | 37.9 | 87.5 | 87.3 | 72.0 | 71.8 |
| Biomass input (50 wt% moisture) [kg/s] | 4.427 | 4.438 | - | - | 2.337 | 2.342 |
| $CO_2$ stream[a] [kg/s] | 1.637 | 1.641 | 1.829 | 1.833 | 0.864 | 0.866 |
| Water to electrolysis [kg/s] | - | - | 2.249 | 2.255 | 1.062 | 1.066 |
| Hydrogen production [kg/s] | - | - | 0.250 | 0.251 | 0.118 | 0.119 |
| Methanol production [kg/s] | 1.252 | 1.255 | 1.252 | 1.255 | 1.252 | 1.255 |
| Bio-methanol [wt%] | 100 | 100 | - | - | 52.8 | 52.8 |
| e-methanol [wt%] | - | - | 100 | 100 | 47.2 | 47.2 |

All flow rates relative to 1 kg/s OME3-5 production.

[a]For bio-OME: vented from process; for e-OME: input to methanol synthesis; for hybrid-OME: recovered from gas treatment in biomass gasification plant and used as input to (e-)methanol synthesis.

# 3 | RESULTS AND DISCUSSION

## 3.1 | Material balance and carbon yield

Flow rates of important inputs and intermediates of the six production pathways are summarized in Table 3, relative to 1 kg/s $OME_{3-5}$ production. Note that the $OME_{3-5}$ yield from methanol is slightly higher by route A, leading to lower mass flows compared to route B. For the hybrid pathways, about 47% of the methanol is produced from the $CO_2$ stream separated from the biomass syngas. The carbon yield for the bio-OME pathways (38%) is considerably lower than for the e-OME pathways (87%). The hybrid-OME route considerably increases the carbon yield (72%) compared with the bio-OME pathways, however not coming up to the levels of the e-OME pathways. This is due to a higher carbon loss in the bio-methanol process in relation to the e-methanol process. For the hybrid process, both bio- and e-methanol processes are operated in parallel, leading to a higher carbon loss from biomass to methanol for the hybrid pathway than from $CO_2$ to methanol for the electricity-based pathway.

## 3.2 | Energy demand

The complete thermal stream data of the six production pathways are available in the Appendix S1. Results of pinch

analysis for the bio- and hybrid pathways are discussed briefly below, and the results for e-OME production (based on the work by Held et al) are summarized. For a more thorough discussion of the e-$OME_{3-5}$ pathways, the reader is referred to Held et al.[35]

### 3.2.1 | Bio-$OME_{3-5}$

The Grand Composite Curves (GCCs) of the two subprocesses (biomass to methanol and methanol to $OME_{3-5}$) are presented in Figure 2A,C,D, and the GCC of the integrated process (colocation of the two subprocesses) is presented in Figure 2E. For the bio-methanol plant and the integrated process, the integration of a steam-cycle for power production and the power generation target determined by pinch analysis are indicated in the corresponding subfigures. The methanol to $OME_{3-5}$ process is heat deficit (minimum heating demand: 0.23 MW per MW $OME_{3-5}$ for the direct route and 0.19 MW per MW $OME_{3-5}$ for the indirect route, see Figure 2C,D, respectively) while the biomass to methanol process has a significant surplus of heat at high temperatures (see Figure 2A). In the stand-alone configuration, excess heat cannot be transferred from the gasification process to the $OME_{3-5}$ process, meaning the entire process chain has an external heat demand corresponding to the minimum heating

**FIGURE 2** Grand composite curves (GCCs) of a selection of the investigated processes (red lines). Integrated steam cycles are indicated by blue lines. Targets for hot utility consumption and power generation are indicated by red and blue arrows, respectively. A global $\Delta T_{min}$ of 10 K has been used for all curves. (A) Stand-alone bio-methanol; (B) stand-alone hybrid-methanol; (C) stand-alone $OME_{3-5}$ (Route A); (D) stand-alone $OME_{3-5}$ (Route B); (E) integrated bio-$OME_{3-5}$ (Route B); (F) integrated hybrid-$OME_{3-5}$ (Route B)
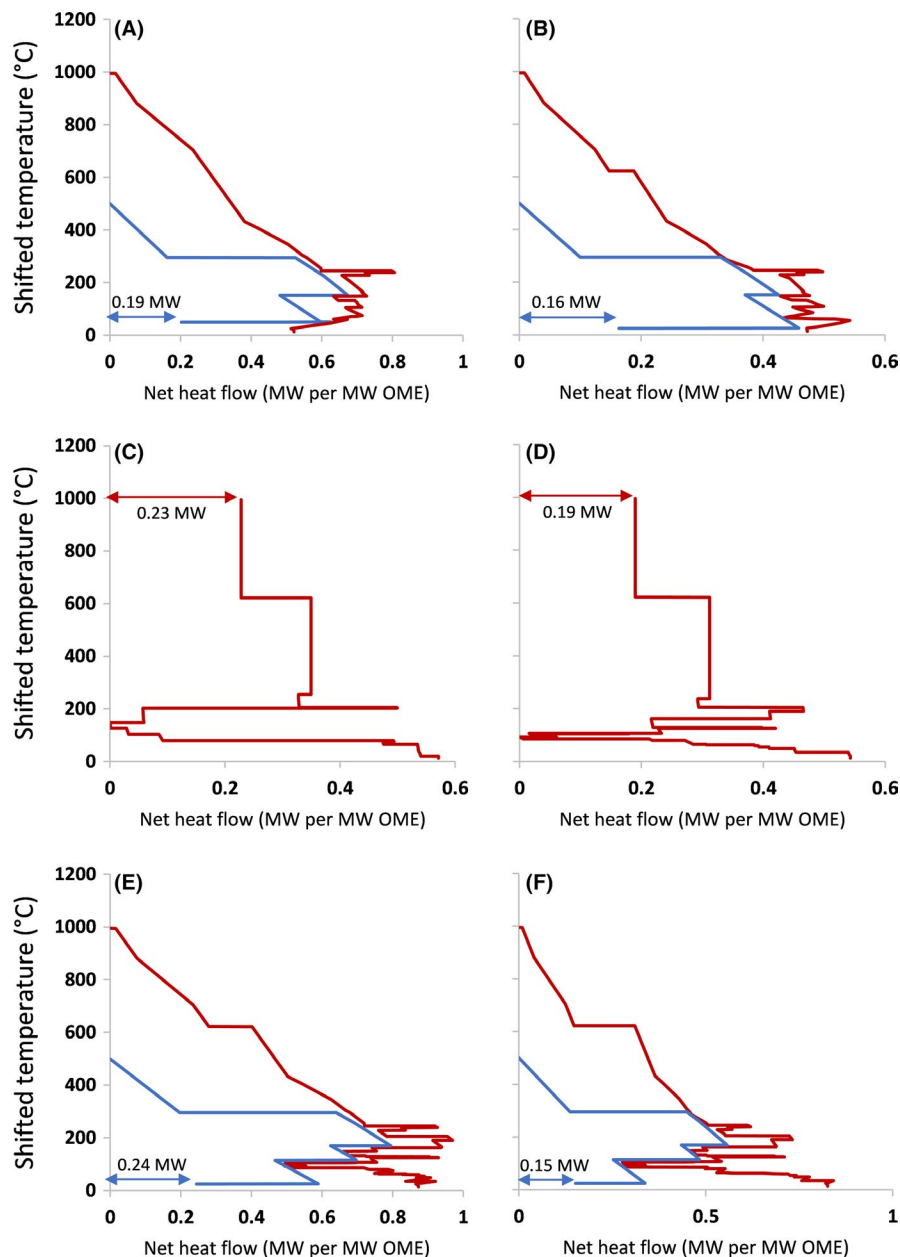


demand of the methanol to $OME_{3-5}$ process. In the integrated process, the external heating demand can be reduced to zero (see Figure 2E). In the stand-alone biomass to methanol plant, as well as in the fully integrated plant, the excess heat from gasification can be used to raise high pressure steam for use in a combined heat and power plant. The on-site power production is enough to meet the power demand of the entire biomass to $OME_{3-5}$ production chain, and for the integrated case proceeding by the indirect route, there is a net power surplus.

### 3.2.2 | e-$OME_{3-5}$

According to the work by Held et al,[35] the production of 1 MJ $OME_{3-5}$ (LHV 19.2 MJ/kg) requires about 2.7 MJ of

electric power and 0.2-0.4 MJ of heat, assuming that the required $CO_2$ is provided by carbon capture from flue gases. The heat demand depends on the level of heat integration and on the process route employed for conversion of methanol to $OME_{3-5}$.

### 3.2.3 | Hybrid-$OME_{3-5}$

The GCCs of the hybrid processes are presented in Figure 2. Figure 2B presents the GCC for stand-alone production of hybrid-methanol (ie, production of methanol from biomass and the $CO_2$ stream from biomass gasification), while Figure 2F presents the GCCs of the integrated production pathway proceeding via the indirect route. Like the bio-$OME_{3-5}$ process, the hybrid-$OME_{3-5}$ process has significant excess heat from

biomass gasification. However, utilization of the $CO_2$ stream from the biomass gasification plant leads to higher $OME_{3-5}$ yield per kilo biomass fed and, consequently, to decreasing gasification excess heat per $OME_{3-5}$ output. This affects the target for on-site power generation, as is illustrated in Figure 2F, representing the integrated hybrid-$OME_{3-5}$ process using the indirect conversion route (Case *Hybrid-OME-B-Int*). The target for on-site power production is 0.15 MW per MW $OME_{3-5}$, which can be compared to 0.24 MW per MW $OME_{3-5}$ for the integrated bio-$OME_{3-5}$ process using the indirect conversion pathway (*Bio-OME-B-Int*, see Figure 2E). Further, the use of hydrogen from electrolysis for part of the methanol generation leads to a significantly higher power demand compared to the bio-$OME_{3-5}$ process.

### 3.2.4 | Comparison of energy demand

The required net energy inputs of biomass, heat, and power are summarized in Figure 3 for the different production concepts (bio-, e-, and hybrid $OME_{3-5}$), conversion routes (direct and indirect), and levels of heat integration (integrated or stand-alone). The highest energy efficiency is achieved by the bio-pathway (45.5%-52.8%, depending on process configuration), followed by the hybrid pathway (40.7%-44.4%) and the electro-pathway (32.7%-33.7%). The effect of integrating methanol and OME production is most pronounced for the bio- and hybrid processes, where heat demand can be reduced to zero (mostly due to utilization of gasification excess heat). While on-site power generation is enough for covering process power demand for all bio-based process configurations, the highest achieved power export is only 0.05 MJ/MJ$_{OME3-5}$ (case *Bio-OME-B-Int*).

Note that the energy efficiency of the indirect route (route B) is slightly higher than that of the direct route (route A), despite the slightly lower yields (see Table 3). This is explained by the lower heat demand of route B, which leads either to possibilities for increased on-site power generation (integrated bio- and hybrid cases) or decreased demand for imported heat (all remaining cases).

### 3.3 | Greenhouse gas emissions

The well-to-tank GHG emissions of bio-, e-, and hybrid-$OME_{3-5}$ have been assessed according to RED II guidelines using the process mass and energy balances described above, the transportation mix given in Table 2 and assumptions given in the Methodology section. Detailed calculations are included in the Appendix S1. Results are presented in Figure 4 and compared to the standard value given in RED II Annex V for Fischer-Tropsch (FT) diesel production using wood chips from forest residues

(8.51 gCO$_{2eq}$/MJ$_{FT-diesel}$). For clarity, and because of the similarity in mass- and energy balance of routes A and B (see Table 3 and Figure 3), results are given only for the slightly more energy-efficient route B. Note that the FT-diesel reference value has been adjusted to be compatible with the biomass transport vector assumed in the present work. Also indicated in Figure 4 are the 65% and 70% GHG reduction levels required for counting of biofuels and nonbiofuels, respectively, toward the renewable fuel target under RED II (corresponding to 32.9 and 28.2 gCO$_{2eq}$/MJ$_{fuel}$, respectively).

All process routes lead to a reduction in GHG emissions by more than 70% compared with the fossil fuel comparator and are therefore compliant with required RED II levels. The $CO_{2eq}$ emissions associated with external heat supply are dominant for all stand-alone pathways. The only pathway achieving a larger GHG emission reduction than the reference value for renewable FT-diesel from forest residues given in Annex V of RED II is integrated hybrid-$OME_{3-5}$, achieving a 92.8% emission reduction (corresponding to 6.74 gCO$_{2eq}$/MJ$_{OME3-5}$). For integrated bio-$OME_{3-5}$, results are comparable to the FT-diesel reference. Process integration for the e-OME pathway does not lead to sufficient heat energy savings to reduce the carbon footprint of external process heat supply. The contribution of transportation GHG emissions is higher for the bio- and hybrid-$OME_{3-5}$ pathways, due to the transport demand of biomass feedstock. For the integrated bio- and hybrid-OME pathways, GHG emissions related to biomass harvesting and processing are the smallest contribution to overall GHG emissions. The GHG emissions of the integrated bio-$OME_{3-5}$ pathway (10.56 g $CO_{2eq}$/MJ) are similar to other advanced biofuel alternatives studied earlier. GHG emission for 2-ethylhexanol produced via syngas from biomass gasification, for example, have been estimated to be 11 g $CO_{2eq}$/MJ.[8] Note however that final distribution is not included in this value and that the inclusion of this term would raise well-to-tank GHG emissions of 2-ethylhexanol to about 12.5 g CO2$_{eq}$/MJ.

## 4 | SENSITIVITY ANALYSIS

Given the significant power demand of the e-$OME_{3-5}$ production process, it is of interest to explore the effect of increasing carbon intensity of the power supply. In Figure 5, the GHG emissions have been recalculated assuming that electricity is supplied from the Swedish grid (average carbon intensity of 13.1 g $CO_{2eq}$/MJ$_{el}$[48]). In this scenario, the $CO_2$ emissions of power supply alone are enough to bring e-$OME_{3-5}$ above the 28.2 g $CO_{2eq}$/MJ limit (corresponding to 70% reduction) required for fuels of nonbiological origin to be counted toward the renewable targets under RED II. As the pure biomass-based pathways all have a net zero or

**FIGURE 3** Net energy input and total energy efficiency for the investigated production pathways, conversion routes, and levels of heat integration. Net energy input of biomass, heat, and power is measured toward the left *y*-axis. Negative numbers indicate a net export. The total energy input is given above the stacked bars for each case. This number corresponds to the denominator of Equation (1) and includes net power imports but does not account for net power exports. The total energy efficiency according to Equation (1) is indicated by rhomboids and measured toward the right *y*-axis. The efficiency is also given (in parentheses) above the stacked bars for each case
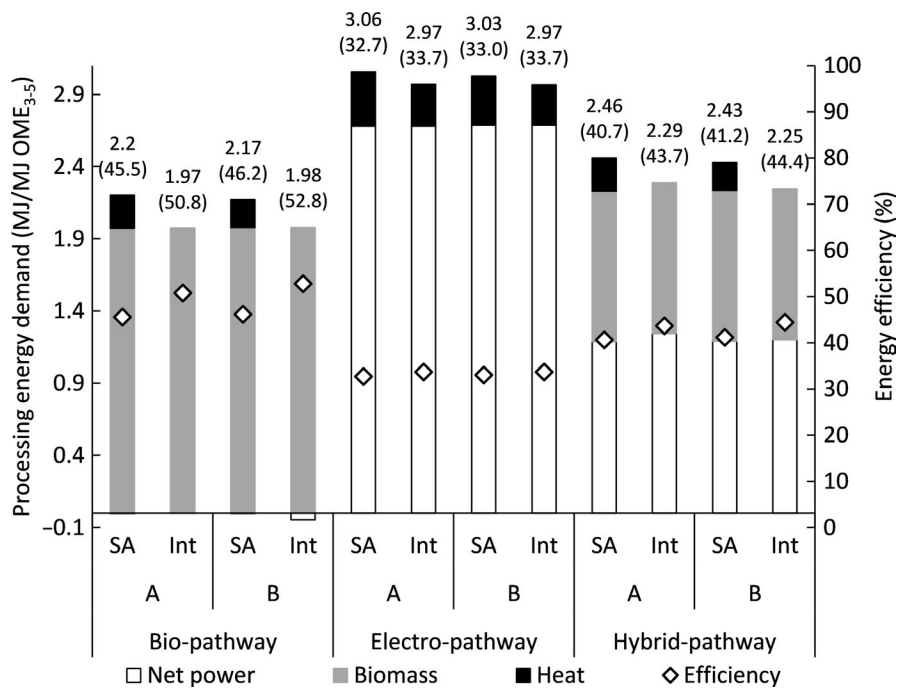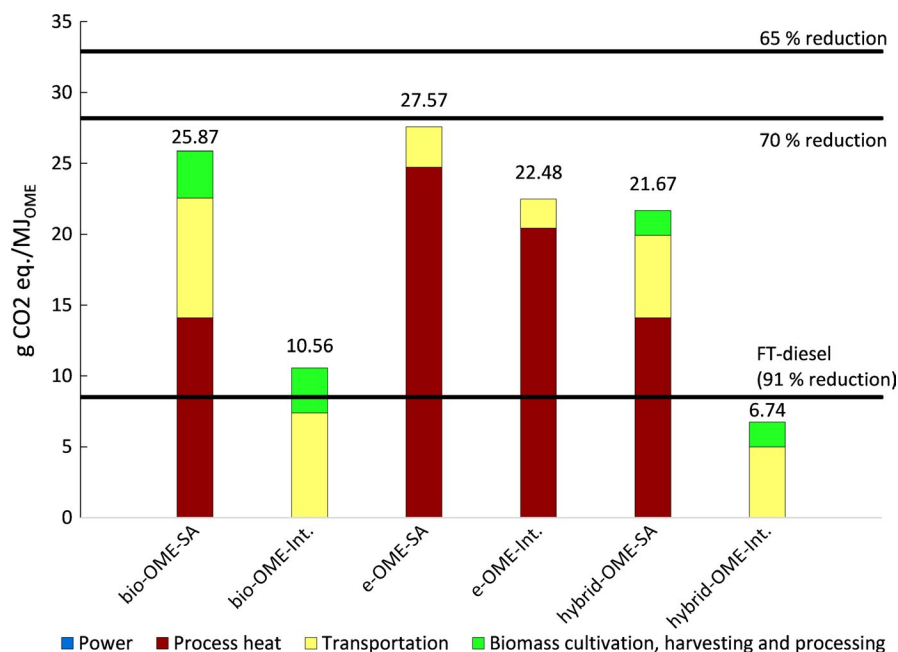


**FIGURE 4** GHG emissions for the production of 1 MJ of $OME_{3-5}$, evaluated according to RED II methodology. Renewable electricity (0 g $CO_{2eq}/MJ_{el}$) is used for power supply, and a natural gas fired boiler is used for heat supply. All results are for route B



export of power, they are nonsensitive to changes in carbon intensity of the power supply, with respect to the GHG emissions. In this scenario, the integrated bio-$OME_{3-5}$ pathway outperforms the integrated hybrid-$OME_{3-5}$ process that is penalized by the emissions related to power demand.

For e-$OME_{3-5}$ and nonintegrated bio- and hybrid-$OME_{3-5}$, emissions associated with heat supply make a large contribution to the overall carbon footprint. Significant reductions to GHG emissions are achieved if a renewable heat source can be used. A scenario using Swedish grid electricity for power supply and biomass for heat supply has been considered, and

results are presented in Figure 6. A biomass boiler firing wood chips from forest residues at 85% thermal efficiency (on fuel LHV) is assumed, and all emissions related to provision and use of this biomass (4.94 g $CO_{2eq}/MJ_{biomass}$, based on[46] and[47]; details are available in the Appendix S1) are attributed to process heat in Figure 6.

A reduction in GHG emission intensity of the heat supply drastically reduces the beneficial effects of process integration, with the stand-alone alternatives resulting in similar GHG emission as the integrated pathways. Given the carbon intensity of the power supply, no pathway can achieve higher GHG emission reductions than the reference fuel
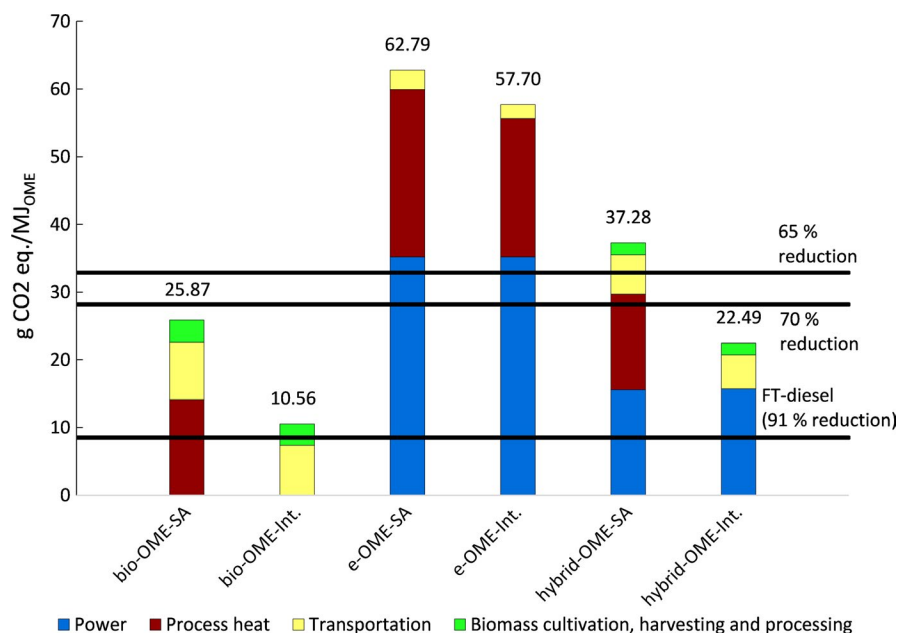
**FIGURE 5** GHG emissions for the production of 1 MJ of $OME_{3-5}$, evaluated according to RED II methodology. Swedish grid electricity is used for power supply, and a natural gas fired boiler is used for heat supply. All results are for route B
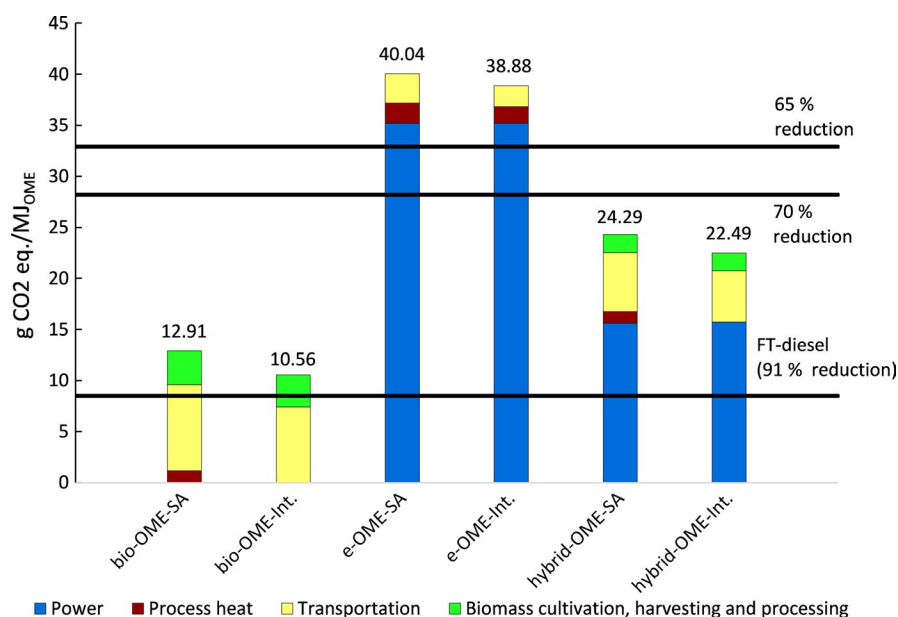


**FIGURE 6** GHG emissions for the production of 1 MJ of $OME_{3-5}$, evaluated according to RED II methodology. Swedish grid electricity is used for power supply, and a biomass-fired boiler is used for heat supply. All results are for route B

FT-diesel. As illustrated in Figure 6, the major contribution to GHG emissions for the $e$-$OME_{3-5}$ pathways stems from power supply in that scenario. Assuming renewable electricity generation with a zero-carbon footprint in combination with biomass-based heat supply, the e-OME pathways clearly perform best.

## 5 | CONCLUSIONS

Six different pathways for $OME_{3-5}$ production have been analyzed for energy efficiency, carbon yield, and GHG emissions. Bio-$OME_{3-5}$ has been demonstrated to be most energy-efficient but resulting in the lowest carbon yield. e-$OME_{3-5}$ has a considerably lower energy efficiency but

results in high carbon efficiency. Combining both pathways into a hybrid-$OME_{3-5}$ process, making use of the separated $CO_2$ from the biomass to methanol process, results in a higher carbon yield than bio-$OME_{3-5}$ at the expense of losses in energy efficiency. Colocation of the methanol production process and the methanol to $OME_{3-5}$ process allows for improving the energy efficiency by process integration in particular for the bio- and hybrid-$OME_{3-5}$ pathways. If renewable electricity is used, GHG emission reductions in comparison with fossil diesel for all investigated $OME_{3-5}$ pathways are above 70%. Assuming natural gas as source of external process heat supply, process integration has a significant impact on the carbon footprint of the bio- and hybrid-OME pathways. Renewable electricity with zero-carbon footprint is a prerequisite for e-$OME_{3-5}$

to be a viable alternative for effective GHG emission reduction. The emission reduction in bio-OME$_{3-5}$ estimated in the present study is similar to other advanced biofuel alternatives, such as 2-ethylhexanol (2-EH). OME$_{3-5}$ can be considered a viable alternative for GHG emission reduction that can be adapted to local energy system conditions to provide the best performance given the carbon intensity of the relevant energy services. The high degree of miscibility with fossil diesel and the possibility for combined reduction in NO$_x$ and soot emissions make it a very attractive fuel candidate for short- to medium-term reductions of CO$_2$ emissions from the transportation sector.

## ACKNOWLEDGMENTS

## ORCID

*Pontus Bokinge* 🔟 https://orcid.org/0000-0003-0619-5091

## ENDNOTE

[1] Calculated for the following composition and individual heating values: 43 wt% OME$_3$ (LHV 19.8 MJ/kg), 34 wt% OME$_4$ (LVH 19.0 MJ/kg), 22 wt% OME$_5$ (18.4 MJ/kg) and 1 wt% OME$_6$ (18.0 MJ/kg).

## REFERENCES

1. European Commission. *Roadmap to a Single European Transport Area - Towards a Competitive and Resource Efficient Transport System*. Brussels, Belgium: European Commission; 2011.
2. Johansson TB, ed. *Fossilfrihet På Väg*. Stockholm, Sweden; 2013. SOU 2013:84.
3. Gutzmer P, Goericke D *Energy Paths for Road Transport in the Future – Options for Climate-Neutral Mobility in 2050*. Frankfurt a.M., Germany: FVV; 2018.
4. U.S. Department of Energy. *Co-Optimization of Fuels & Engines*. https://www.energy.gov/eere/bioenergy/co-optimization-fuels-engines. Accessed November 20, 2019.
5. RWTH Aachen University. *Fuel Science Centre*. https://www.fuelcenter.rwth-aachen.de/go/id/siul/?lidx=1. Accessed November 20, 2019.
6. Preuß J. Future fuels for transportation. In: *Energirelaterad Fordonsforskning (Energy-Related Automotive Research)*. Gothenburg, Sweden: Swedish Energy Agency; 2019.
7. König A, Ulonska K, Mitsos A, Viell J. Optimal applications and combinations of renewable fuel production from biomass and electricity. *Energy Fuels*. 2019;33(2):1659-1672.
8. Poulikidou S, Heyne S, Grahn M, Harvey S. Life-cycle energy and greenhouse gas emissions analysis of biomass-based

9. Burger J, Ströfer E, Hasse H. Chemical equilibrium and reaction kinetics of the heterogeneously catalyzed formation of poly(oxymethylene) dimethyl ethers from methylal and trioxane. *Ind Eng Chem Res*. 2012;51(39):12751-12761.
10. Niethammer B, Wodarz S, Betz M, et al. Alternative liquid fuels from renewable resources. *Chem Ing Tec*. 2018;1:99-112.
11. Oyedun AO, Kumar A, Oestreich D, Arnold U, Sauer J. The development of the production cost of oxymethylene ethers as diesel additives from biomass. *Biofuels Bioprod Biorefin*. 2018;12(4):694-710.
12. Pellegrini L, Marchionna M, Patrini R, Beatrice C, Del Giacomo N, Guido C. *Combustion Behaviour and Emission Performance of Neat and Blended Polyoxymethylene Dimethyl Ethers in a Light-Duty Diesel Engine*. SAE Technical Paper. 2012-01-1053; 2012.
13. Mahbub N, Oyedun AO, Kumar A, Oestreich D, Arnold U, Sauer J. A life cycle assessment of oxymethylene ether synthesis from biomass-derived syngas as a diesel additive. *J Clean Prod*. 2017;165:1249-1262.
14. Hackbarth K, Haltenort P, Arnold U, Sauer J. Recent progress in the production, application and evaluation of oxymethylene ethers. *Chem Ing Tec*. 2018;90(10):1520-1528.
15. Burger J, Siegert M, Ströfer E, Hasse H. Poly(oxymethylene) dimethyl ethers as components of tailored diesel fuel: properties, synthesis and purification concepts. *Fuel*. 2010;89(11):3315-3319.
16. Deutz S, Bongartz D, Heuser B, et al. Cleaner production of cleaner fuels: wind-to-wheel – environmental assessment of CO$_2$-based oxymethylene ether as a drop-in fuel. *Energy Environ Sci*. 2018;11(2):331-343.
17. Breitkreuz CF, Schmitz N, Ströfer E, Burger J, Hasse H. Design of a production process for poly(oxymethylene) dimethyl ethers from dimethyl ether and trioxane. *Chem Ing Tec*. 2018;90(10):1489-1496.
18. Schmitz N, Ströfer E, Burger J, Hasse H. Conceptual design of a novel process for the production of poly(oxymethylene) dimethyl ethers from formaldehyde and methanol. *Ind Eng Chem Res*. 2017;56(40):11519-11530.
19. Zhang X, Kumar A, Arnold U, Sauer J. Biomass-derived oxymethylene ethers as diesel additives: a thermodynamic analysis. *Energy Procedia*. 2014;61:1921-1924.
20. Lautenschütz L, Oestreich D, Seidenspinner P, Arnold U, Dinjus E, Sauer J. Physico-chemical properties and fuel characteristics of oxymethylene dialkyl ethers. *Fuel*. 2016;173:129-137.
21. Baranowski CJ, Bahmanpour AM, Kröcher O. Catalytic synthesis of polyoxymethylene dimethyl ethers (OME): a review. *Appl Catal B*. 2017;217:407-420.
22. Wang D, Zhu G, Li Z, Xia C. Polyoxymethylene dimethyl ethers as clean diesel additives: fuel freezing and prediction. *Fuel*. 2019;237:833-839.
23. Li D, Gao Y, Liu S, Ma Z, Wei Y. Effect of polyoxymethylene dimethyl ethers addition on spray and atomization characteristics using a common rail diesel injection system. *Fuel*. 2016;186:235-247.
24. Liu H, Wang Z, Li Y, Zheng Y, He T, Wang J. Recent progress in the application in compression ignition engines and the synthesis technologies of polyoxymethylene dimethyl ethers. *Appl Energy*. 2019;233-234:599-611.

25. Wang Z, Liu H, Ma X, Wang J, Shuai S, Reitz RD. Homogeneous charge compression ignition (HCCI) combustion of polyoxymethylene dimethyl ethers (PODE). *Fuel*. 2016;183:206-213.

26. Liu H, Wang Z, Wang J, et al. Performance, combustion and emission characteristics of a diesel engine fueled with polyoxymethylene dimethyl ethers (PODE3-4)/diesel blends. *Energy*. 2015;88:793-800.

27. Burger J, Ströfer E, Hasse H. Production process for diesel fuel components poly(oxymethylene) dimethyl ethers from methane-based products by hierarchical optimization with varying model depth. *Chem Eng Res Des*. 2013;91(12):2648-2662.

28. Weidert J-O, Burger J, Renner M, Blagov S, Hasse H. Development of an integrated reaction-distillation process for the production of methylal. *Ind Eng Chem Res*. 2017;56(2):575-582.

29. Lang N, Ströfer E, Stammer A, et al. *Integrated Process For Preparing Trioxane From Formaldehyde*. 2005. United States Patent US20080194845A1; 2008.

30. Siegert M, Lang N, Ströfer E, Stammer A, Friesse T, Hasse H. *Method for separating trioxane from a trioxane/formaldehyde/water mixture by means of pressure change rectification*. 2007. United States Patent US20070272540A1; 2007.

31. Wang D, Zhu G, Li Z, Xue M, Xia C. Conceptual design of production of eco-friendly polyoxymethylene dimethyl ethers catalyzed by acid functionalized ionic liquids. *Chem Eng Sci*. 2019;206:10-21.

32. Wang D, Zhao F, Zhu G, Xia C. Production of eco-friendly poly(oxymethylene) dimethyl ethers catalyzed by acidic ionic liquid: a kinetic investigation. *Chem Eng J*. 2018;334:2616-2624.

33. Burre J, Bongartz D, Mitsos A. Production of oxymethylene dimethyl ethers from hydrogen and carbon dioxide—part II: modeling and analysis for OME3–5. *Ind Eng Chem Res*. 2019;58(14):5567-5578.

34. Zheng Y, Tang Q, Wang T, Liao Y, Wang J. Synthesis of a green fuel additive over cation resins. *Chem Eng Technol*. 2013;36(11):1951-1956.

35. Held M, Tönges Y, Pélerin D, Härtl M, Wachtmeister G, Burger J. On the energetic efficiency of producing polyoxymethylene dimethyl ethers from CO$_2$ using electrical energy. *Energy Environ Sci*. 2019;12(3):1019-1034.

36. Shan J, Lucci FR, Liu J, et al. Water co-catalyzed selective dehydrogenation of methanol to formaldehyde and hydrogen. *Surf Sci*. 2016;650:121-129.

37. Zhang X, Oyedun AO, Kumar A, Oestreich D, Arnold U, Sauer J. An optimized process design for oxymethylene ether production from woody-biomass-derived syngas. *Biomass Bioenerg*. 2016;90:7-14.

38. Tunå P, Hulteberg C. Woody biomass-based transportation fuels – A comparative techno-economic study. *Fuel*. 2014;117(PART B):1020-1026.

39. Holmgren KM, Berntsson T, Andersson E, Rydberg T. System aspects of biomass gasification with methanol synthesis – process concepts and energy analysis. *Energy*. 2012;45(1):817-828.

40. Andersson J, Lundgren J, Marklund M. Methanol production via pressurized entrained flow biomass gasification – techno-economic comparison of integrated vs. stand-alone production. *Biomass Bioenerg*. 2014;64(11):256-268.

41. Joelsson JM, Engström C, Heuts L. *From Green Forest to Green Commodity Chemicals*. Stockholm, Sweden: Vinnova – Swedish Governmental Agency for Innovation Systems; 2015.

42. Morandin M, Harvey S. *Methanol via Biomass Gasification - Thermodynamic Performance and Process Integration in Swedish Chemical Clusters and Pulp and Paper Sites*. Gothenburg, Sweden; 2014.

43. Andersson E, ed. *Skogskemi – Gasification Platform. Sub Project Report to the Skogskemi Project*. Örnsköldsvik, Sweden: SP Processum AB; 2014.

44. Linnhoff B, Townsend DW, Boland D, et al. *User Guide on Process Integration for the Efficient Use of Energy. Revised 1s*. Rugby, UK: IChemE; 1994.

45. Kemp IC. *Pinch Analysis and Process Integration: A User Guide on Process Integration for the Efficient Use of Energy*, 2nd ed. Oxford, UK: Butterworth-Heinemann; 2007.

46. The European Parliament and the Council of the European Union. Directive (EU) 2018/2001 of the European Parliament and of the Council on the Promotion of the Use of Energy from Renewable Sources; 2018. https://eur-lex.europa.eu/legal-content/EN/TXT/PDF/?uri=CELEX:32018L2001&from=EN. Accessed November 22, 2019.

47. Edwards R, O'Connell A, Padella M, et al. *Definition of Input Data to Assess GHG Default Emissions from Biofuels in EU Legislation, Version 1d-2019*. EUR 28349 EN. Luxembourg: Publications Office of the European Union; 2019.

48. Moro A, Lonza L. Electricity carbon intensity in European Member States: impacts on GHG emissions of electric vehicles. *Transp Res Part D: Transp Environ*. 2018;64:5-14.

## SUPPORTING INFORMATION

Additional supporting information may be found online in the Supporting Information section.